Predictions of Climate following Volcanic Eruptions

Matthew Collins, Centre for Global Atmospheric Modelling, Department of Meteorology, University of Reading, Reading, RG6 6BB, UK. matcollins@met.rdg.ac.uk

Abstract

Predictions of climate for seasons and years into the future can be of considerable benefit to society. While large explosive volcanic eruptions may not be predictable with any confidence on these time scales, once the eruption has occurred the climate impact may be exploited to provide a climate forecast. In this paper, retrospective forecasts of the climate impacts of the 1982 eruption of El Chichón and the 1991 eruption of Pinatubo are examined to quantify the potential accuracy of such forecasts. Recognizing that there is no single pre-determined climate path following an eruption, and that all climate forecasts are essentially probabilistic in nature, it is shown that volcanoes of the size of El Chichón and Pinatubo can significantly bias the probability of occurrence of anomalies in climate variables such as surface air temperature and mean sea level pressure. However, the volcanic signal is only robust on the spatial scale of continents and, moreover, the signal can easily be contaminated or completely obscured by climate variability which is independent of the volcanic perturbation. It is not simply enough to issue a forecast of the form "winter will be warmer and summer will be cooler" following an eruption. Care must be taken and forecasts should explicitly quote probability levels. However it is recommended that forecasting centers develop the capacity to forecast climate following the next big eruption.

Introduction

The chaotic nature of atmospheric motions means that it is impossible to make weather forecasts for many months into the future [e.g. *Lorenz,* 1982]. Weather forecasts exhibit "sensitive dependence on initial conditions" which means that two weather forecasts that start from indistinguishable atmospheric states, while remaining close for perhaps several days, eventually diverge from each other and result in two very different future weather patterns. This sensitive dependence on initial conditions means that even if one could make perfect observations of the current state of the atmosphere and introduce them perfectly into a perfect weather forecast model, it is impossible to predict the exact weather e.g. a week ahead. By defining "climate" as the aggregated effects of weather (in both space and time) it is easy to see that climate forecasts will also exhibit sensitive dependence on initial conditions: Given an initial estimate of the state of the climate system (atmosphere, ocean, biosphere, cryosphere etc.) today, it is not possible to predict e.g. the precise winter mean temperature for next year.

Climate forecasts are thus inherently probabilistic. A typical climate forecast might be of the form "there is a 75% chance of cooler than average temperatures in Western Europe next summer". An important concept in climate forecasting is that for each climate variable, such as Western European summer temperature, there is a *climatological probability density function* (PDF – fig. 1) from which the observed temperature will be drawn. The chaotic nature of the system means that there is no way of knowing from what region of the PDF the observations will be drawn from. There are two principal ways in which climate predictability (i.e. the ability to make climate predictions) may occur [*Lorenz,* 1975]. Predictability may arise when, under certain conditions, climate trajectories diverge less rapidly than they do on average, resulting in a *forecast probability density function* that is "thinner" than the climatological PDF. This is a first kind or initial value climate forecasting problem, a typical example being a forecast of the El Niño phenomena in which there is a smaller than average probability of a medium to large warm or cold event and forecast trajectories remain close to normal conditions. Predictability of the second kind arises when the forecast PDF is shifted with respect to the climatological PDF resulting in, for example, a significant increase in the occurrence of

normally low probability events such as floods or droughts in comparison to normal. By introducing a significant perturbation to the energetic balance of the climate system, a volcanic eruption can shift the climate PDF in this manner and pave the way for making climate forecasts [*Robock*, 2001]. Even if the eruption itself is completely unpredictable, once it has occurred the resulting perturbation may be exploited.

Amongst the most effective eruptions that can cause significant shifts in the PDFs of climate variables are those that inject large amounts of SO_2 into the Stratosphere, which is in turn converted to sulphate aerosol, resulting in a perturbation to the radiative balance of the system. This paper examines two such cases, the eruption of El Chichón in March-April 1982 and the eruption of Pinatubo in June 1991. Both eruptions are reasonable well observed in terms of their stratospheric aerosol loading [*Strong*, 1984; *Bluth et al.*, 1992; *Stowe et al.*, 1992], and thus provide suitable test-beds for the examination of the potential for climate forecasting. Hindcasts (i.e. retrospective forecasts) of the climatic impacts of the eruptions are made using a numerical model of the climate system that simulates the dynamical evolution of both the ocean and the atmosphere. Such numerical models are widely used in climate science and are at the core of, e.g., projections of future anthropogenic climate change [*Houghton et al.*, 2001]. Because of the probabilistic nature of climate forecasts, it is not sufficient to perform a single simulation of an eruption in order to assess its impact on climate and its potential for forecasting. An ensemble of many simulations is required, starting from different initial conditions, in order to assess probabilities. Chaos means that following a volcanic eruption, there is no single pre-determined pathway that the climate system will follow. There are a number of different pathways, including (as we shall see) pathways in which other climatic phenomena may contaminate or even mask the volcanic signal.

The considerable effort made in developing El Niño forecasting systems has had produced many benefits to society, such as early warnings of drought conditions and there subsequent impact on agriculture. The oceanic El Niño and its atmospheric component the Southern Oscillation (together termed ENSO) remains the “weapon of choice” for climate forecasters. Efforts to predict other climate phenomena such as the North Atlantic Oscillation are still rather experimental and reliable forecasts of regions that are not influenced by ENSO have yet to be established. The exploitation of volcanic eruptions to make predictions of climate might produce significant benefits to society. It is the purpose of this paper to quantify how useful they might potentially be.

Methods

Modelling

The model used is version three of the Hadley Centre for Climate Prediction and Research coupled atmosphere ocean model – HadCM3 [*Gordon et al.*, 2000; *Collins et al.*, 2001]. The ocean component of the model has a horizontal resolution of 1.25º longitude by 1.25º latitude and has 20 levels in the vertical from the surface to the bottom of the ocean. The atmospheric component of the model has a horizontal resolution of 3.75ºx2.5º in longitude and latitude with 19 unequally spaced vertical levels from the surface up to approximately 40km, with 6 levels representing the Stratosphere. The two components are coupled without the use of artificial flux corrections and the model has a stable surface climate.

Aerosol distributions associated with both El Chichón and Pinatubo are taken from an updated version of the *Sato et al.* [1993] dataset and are introduced into the model in four uniform latitudinal bands from 90°S-45°S, 45°S-equator, equator-45°N and 45°N-90°N. The representation of the volcanic forcing by such broad spatial scales in part reflects the uncertainty there would be in the transport of aerosol particles by chaotic stratospheric dynamics following an eruption. A potential improvement to this study, and a component of any operational forecasting system, would be the inclusion/prediction of a more realistic pattern of aerosol loading. Given the chaotic nature of atmospheric dynamics and the large-scale pattern of the response, quite

how accurate this forcing needs to be to result in useful climate forecasts is still an open question. The net radiative forcing (i.e. the change in the radiative balance of the model) resulting from the inclusion of the *Sato et al.* [1993] aerosol optical depths are shown in fig. 2. The net forcing is composed of two components, a negative (i.e. surface/troposphere cooling) shortwave component resulting from the direct reduction of incoming solar radiation by the aerosol particles, and a positive (i.e. surface/troposphere warming) longwave component resulting from the enhanced greenhouse effect of the aerosol particles. In each case, the former of these effects dominates and the general pattern of forcing is negative, although there is some small positive forcing in the polar night regions at times when there is no incident solar radiation hence no shortwave effect. *Stenchikov et al.* [1998] and *Andronova et al.* [1999] present a much more extensive study of the radiative effects of volcanic eruptions.

The radiative forcing associated with the Pinatubo eruption is larger and more long-lived than that associated with El Chichón simply because of the greater amount of SO_2 released into the stratosphere during that eruption (20 *Mt* in comparison with 7 *Mt* [*Bluth et al.*, 1992]). In addition, the forcing pattern for Pinatubo is more global in extent, whereas the El Chichón forcing pattern is more confined to the northern hemisphere. The magnitude of the forcing is of the order of several Wm^2, which is similar to that associated with a doubling of CO_2, but because of the relatively short lifetime of the aerosol particles in the atmosphere, the impact of the eruption on global climate is correspondingly short (see figs 5 and 6).

The effects of increasing greenhouse gases, solar variability and athropogenic aerosols are also included in the simulations [*Stott et al.*, 2001]. The time scales for climate perturbations associated with these forcings are decadal and longer, hence we may assume that their effects are unimportant for the seasonal to interannual time scales examined here. Long-term trends (in both the observations and the model experiments) must however be taken into account when defining the base period from which to compute climate and forcing anomalies. In each case, the five years prior to the year of the eruption are used to define the climatology from which anomalies are computed.

An ensemble of 20 simulations is performed for both eruptions in order to assess probabilities. The simulations use four different oceanic initial states and 20 different atmospheric initial states [*Collins et al*, 2002] in order to sample uncertainty in both components of the climate system. The ocean initial state is the crucial one for the first kind or initial value prediction problem, but here no attempt is made to produce an initial state that is consistent with the observed ocean state prior to either eruption. In addition, simulations are initiated 5-6 years prior to the eruptions in order to minimize any "memory" of the ocean initial conditions. This cleanly separates the effects of initial and boundary conditions and means that *the predictability assessed here is that due to the volcanic boundary forcing only*. In any operational forecasting system, account should be taken of both the initial and boundary conditions [*Collins and Allen*, 2002], but here the focus is on that which comes solely from the boundary forcing.

Data Processing

The focus here is on the prediction of two climate variables. Surface air temperature (SAT) is of direct relevance to society and is directly affected by the radiative perturbation introduced by a volcanic eruption and hence is likely to be significantly perturbed with respect to climatology. Mean Sea Level Pressure (MSLP) is a good indicator of wind strength and direction (in mid-latitudes) and of such phenomena as the North Atlantic Oscillation (NAO – *Hurrell* [1995]). It is not directly influenced by the radiative forcing, but can be influenced indirectly via changes in atmospheric dynamics associated with atmospheric temperature changes. Both SAT and MSLP are known to be reasonably well simulated by global circulation models (GCMs), whereas variables such as precipitation and extreme storms are less skillfully simulated. One of the challenges for making all types of climate forecasts, from seasonal to centenial time scales, is the improvement of GCMs to more accurately simulate variables which are of direct impact on society

Observations of land surface air temperature (ocean temperatures are not considered as they are not so directly relevant to society) are taken from *Jones et al.* [1994]. Data coverage is incomplete and this may influence the comparison with the model fields. The model simulated surface air temperatures at 1.5m are thus first interpolated from the 3.75ºx2.5º model grid to the 5ºx5º observational grid using bilinear interpolation and model grid-boxes for which there are no observed data are also flagged as missing. This allows direct comparison between the model hindcast and the observed data. Because of anthropogenic trends in both the model simulations and in the observations, seasonal mean anomalies are computed with respect to the average conditions for five years prior to the eruption. For the quantitative comparisons performed here and elsewhere, care should always be taken to compute climate anomalies in a consistent manner.

Observations of MSLP are taken from the Global Mean Sea Level Pressure (GMSLP) data set of *Basnett and Parker* [1997]. Again, data coverage is incomplete and the model MSLP is interpolated onto the 5ºx5º observational grid and grid boxes are flagged as missing if there are no observations of MSLP during that particular year and season. MSLP is examined over ocean basins as, in mid-latitudes, these are the main locations of the storm tracks.

In the case of many climate variables, data sets that offer complete global coverage do exist. Regions of missing data are either in-filled using statistical techniques or by taking the so-called re-analysis products of weather forecasting centers, where regions of missing data are in-filled in a more physically consistent way. For this study it is more appropriate to use the raw gridded datasets as, when using the in-filled products, there is the potential for the mis-verification of the hindcast in regions where there are no observations.

Results

Surface Air Temperature

The ensemble mean (the average over all the experiments with different initial conditions) gives an indication of the response of the model to the volcanic radiative forcing, averaging out the random "noise" of climate variations which always occur in addition to the forced component. This is shown for the northern hemisphere winter December to February (DJF) season and the summer June to August (JJA) season in the year immediately after the eruption of El Chichón (fig. 3 – upper panel) and Pinatubo (fig. 4 – upper panel). In both cases the temperature perturbations are of the order of 1-2°C that, while not appearing to be that large in comparison with day-to-day variations in temperature, are in many regions significant in comparison with the normal range of seasonally-averaged temperatures and are comparable with the magnitudes of temperature anomalies found in, for example, simulations of greenhouse gases induced climate change over the next few decades [*Houghton et al.*, 2001].

The model predicts near-global patterns of cooler than average temperatures in the summer seasons following their eruptions, with somewhat stronger anomalies following Pinatubo due to the greater radiative forcing (fig. 2). Small regions of slight warming in the ensemble mean in the summer following El Chichón are simply due to chance and reflect the smaller radiative forcing. For example, the southern hemisphere forcing is only of the order of 1-2Wm^{-2} and hence not large enough to significantly cool the Australian region which is predicted to be slightly warmer than average. (Because of the complex non-linear nature of the climate system, it is not entirely appropriate to relate radiative forcing directly to changes in surface air temperature. However, for global and large-scale patterns, an approximate relationship holds [*Stott et al.*, 2000].) In the winters following the eruptions, the patterns of mean temperature anomalies are more complex. The general pattern of cooling associated with the decrease in net radiative forcing is disrupted by a broad pattern of warming in northern Europe in both cases and over the whole of the northern Eurasian continent in the case of the 1982-3 DJF winter season following El Chichón. This "winter warming" was

first pointed out by *Robock and Mao* [1992] and is thought to be associated with an indirect change in atmospheric circulation that is common following volcanic eruptions (see later).

Comparison of the ensemble mean model response with the observed climate anomalies (figs. 3 and 4 – middle panels) gives some idea of the accuracy of the model in simulating climate anomalies associated with volcanic eruptions, as well as giving some assessment of the potential for making predictions of climate. However, it should be re-iterated that the observations are composed of the response to the volcanic radiative perturbation together with anomalies associated with chance climate fluctuations, and hence when the former are of a similar or lesser order of magnitude than the latter, the agreement will often be far from perfect. However, there are some qualitative agreement between the model ensemble mean hindcasts and the observations. The broad pattern of winter warming in northern Eurasia following El Chichón is captured qualitatively together with a tropic-wide pattern of cooling. The warmer than average temperatures in North America are not predicted by the model and are more likely due to the large El Niño event which occurred concurrently with the volcanic eruption. This is a clear example of how climate noise may obscure the volcanic signal. The model hindcast of near global scale cooling in the summer following El Chichón appears to verify less well with large-scale patterns of warmer than average temperatures observed at that time – again random climate fluctuations can spoil a simple-minded forecast based on the ensemble mean. For Pinatubo, the model predicts a more geographically confined pattern of Eurasian winter warming than actually occurred, although this could also be down to chance. Again, the ensemble mean hindcast does not verify well over North America which is warmer than average in the observations. The summer temperatures following Pinatubo show near global cooler than average temperatures (with the exception of North Western Europe) as indicated by the model ensemble mean. The greater radiative forcing associated with Pinatubo results in a more robust pattern of cooling than was the case for El Chichón.

Performing an ensemble of simulations allows the examination of the PDFs of climate variables following a volcanic eruption. There are many ways to cut the PDF (e.g. into three equal probability tercials or by examining the tails of the distribution for extreme events) all of which are dependent on the particular sensitivities of the individual user of the climate forecast. One of the most simple methods of examining the PDF, is to simply look for anomalies which are either greater or less than the climatological mean (in this case the seasonal mean for the 5 years prior to the eruption). The probability of cooler than average temperatures in the winter and summer seasons following El Chichón and Pinatubo are shown in figs. 3-4 (lower panels). These figures reflect the pattern of response shown in the ensemble mean figures, but also give some indication of the magnitude of the response with respect to the normal climatological variation of surface temperature. They are also the type of forecast map that might be issued following an explosive volcanic eruption. For this type of probability measure, there is a climatological probability of 0.5 and hence the greater the difference between the forecast probability from 0.5, the more confidence there is in the forecast and the greater the chance of the forecast user having to act upon that forecast. For the summer season following both El Chichón and Pinatubo, there is a near global pattern of a greater than average chance of cooler temperatures with probabilities reaching > 0.8 in some regions. As in the ensemble mean, for the winter season the cooler than average pattern is disrupted by a reduced probability (i.e. <0.5) of cooler than average conditions (and hence an increase in the probability of warmer than average conditions) in the northern mid-high latitudes.

The verification of such probabilistic forecasts is difficult as, for example, for a single event such as the prediction of cooler than average temperatures and a reality of warmer than average temperatures, it is impossible to say if this was a bad forecast or if the forecaster was just unlucky. When the forecast and climatological PDF overlap (e.g. fig 1), even if the forecast is biased cold, there may still be a finite probability of warmer than average conditions. In weather forecasting, the usual way of verifying probabilistic forecasts is to consider many such cases and examine the average skill of a forecast system (e.g. by counting the number of 3 day forecasts which were correct). Here only two volcanic eruptions are

considered and it is difficult to make meaningful probabilistic verification scores. However, it is possible to draw some conclusions by averaging over all grid points.

Tables 1 and 2 show a simple form of probabilistic verification skill score for the model hindcasts of El Chichón and Pinatubo. For these measures, i.e. the verification of the sign of the predicted temperature anomaly in 5ºx5º longitude-latitude grid boxes, there are only a few cases in which scores are significantly larger than the 50% score that would be obtained, on average, for a completely random forecast obtained by tossing a coin. For predictions of cooler than average temperatures, there are scores of around 60-70% in the seasons following El Chicon meaning that of all the grid boxes in which the temperature was predicted to be cooler than average, only 60-70% turned out to actually be cooler than average. Skill scores for predictions of cooler than average temperatures are larger following Pinatubo, reaching 86% in the summer of 1992. Verifying predictions of one sign can be misleading as a prediction that stated that all grid boxes were to be cooler than average would result in a skill score of 100%. A more equitable measure is of the number of grid boxes in which the sign of the observed temperature anomaly was predicted correctly (column 5 in tables 1 and 2). These skill scores are in the region of 50% for the El Chichón eruption, and hence similar to what would be obtained by a random forecats, and rise only above the 60% level in the summer and autumn of 1992 following Pinatubo. For this measure, a random forecast would have performed just as well.

There are two potential reasons for these low verification scores. The model may be in error (i.e. the formulation of the model may be incorrect, having both systematic and random errors or there may be errors in the volcanic forcing) or chance climate fluctuations may have obscured the volcanic signal. The former source of error may be examined by substituting one of the model ensemble members as the truth and recalculating the verification scores. In this way the potential for model error is eliminated by working in a "perfect model" environment. The range of skill scores obtained by substituting each ensemble member in turn is also shown in tables 1-2. In many cases, and in particular for the skill of the prediction of the sign of the anomaly (column 5), the verification of the observed temperature is bounded by the range of perfect model scores. This indicates that the latter source of error dominates: The forecast of the sign of temperature anomalies in 5ºx5º grid boxes is more often spoilt by chance climate fluctuations that mask the volcanic signal than by systematic model errors. However, there is some indication from tables 1-2, that there is still the potential for model improvement.

Because large-scale climate perturbations such as volcanic eruptions produce large-scale patterns of climate anomalies, and because economies are now often organized across many countries, it is perhaps better to examine the skill of the hindcasts averaged over larger geographical regions than at the model grid-scale. It is also the case that, because of the numerical formulation of the fluid dynamical solvers incorporated in GCMs, the model should better represent scales representative of a number of grid-boxes. Time series of a selection of global and large-scale averages of temperature are shown in figs. 5-6 for the ensemble simulations and the observations. Again, the spread of the individual ensemble members highlight the range of potential trajectories that the climate system might follow after the eruption of a volcano – there is no single pre-determined pathway. Indeed, this is clearly highlighted in the case of global mean land surface temperatures following El Chichón (fig 5 upper panel). The ensemble mean of the model simulations suggest a global cooling for 2-3 years following the eruption (as would be expected), whereas the real world produced a global warming. This warming is, in part due to the large El Niño event that occurred at this time (El Niños are associated with warmer than average years globally), but is also due to the large Eurasian warming (fig. 3).

Following El Chichón (fig. 5), there are modest, yet significant, displacements of the PDF of surface air temperature in the summer season for all the large-scale regions shown. For Eurasian land SAT, the mean of the PDF is displaced to –0.3°C which is approximately one standard deviation of the climatological PDF. This results in, for example, a 20% probability of a temperature anomaly of less than –0.5°C and a less than

1% probability of a temperature anomaly of greater than 0.5°C (in comparison with the 4% climatological chance of either). In reality, the mean temperature of the Eurasian continent was about normal, despite the increased probability of cooler than average conditions. This was then a perfectly valid forecast as the observations lie well within the bounds of the forecast PDF – again this highlights the problem of verifying probabilistic forecasts. In the winter season, there are generally smaller shifts of the PDFs with only that for Asian land SAT statistically significant. For Eurasian land SAT there is a small shift towards warmer conditions, but nothing that would suggest a significant increase in the probability of warmer than average conditions. As was seen in fig. 3, Eurasian land SATs were significantly warmer than normal but these ensemble simulations suggest that this could easily be just a chance fluctuation in climate. Winter warming is discussed further below.

Biases in forecast PDFs are larger for the Pinatubo case (fig. 6). For the summer season, the probability of Eurasian land SAT anomalies of less than –0.5°C is 42% and the probability of temperature anomalies of greater than 0.5°C less than 1%. In this case, the observed temperature anomaly was –0.6°C, significantly cooler than climatology. The same is true for the other indices shown, although it is worth noting that this apparently good forecast verification (i.e. negative anomalies when negative anomalies are predicted) could equally be explained by chance fluctuations in climate, as was the poor forecast of winter warming following El Chichón. The key message from figs. 5-6 is that, in order for a definitive forecast such as "a cooler summer will follow a large volcanic eruption" the forecast PDF must be significantly displaced with respect to the climatological PDF. When the forecast PDF and climatological PDF overlap, which is the case for both El Chichón and Pinatubo, even the forecasting of relatively large regional averages such as the Eurasian continent, can be affected by random climate fluctuations which can mask the volcanic signal.

It seems then that the model hindcasts verify better when looking at large-scale averages of temperature. Re-computing the verification skill scores of tables 1 and 2 for overlapping regions of size 25ºx25º longitutude-latitude, leads to better hindcasts of the sign of temperature anomalies with as much as 82% of such regions having the correct sign of anomalies predicted for the summer season following Pinatubo. Model predictions can be much more skillful at these spatial scales, both because models are generally more believable at scales of many grid-boxes and because the volcanic signal is less likely to be obscured by the noise of natural climate fluctuations.

It is clear from the analysis of these experiments that care should be taken in making and interpreting climate forecasts following volcanic eruptions. Even for large eruptions such as Pinatubo, which brought about significant global cooling, the predictions that would have been made with the climate model used here of surface air temperatures at the regional scale (i.e. scales of a few hundreds of kilometers) would have been of little use for those interested in the sign of the temperature anomaly. For larger regions (e.g. continental scale) the situation as more promising as the signal is less likely to be obscured by the noise of natural climate fluctuations. However, for the smaller eruption of El Chichón, this indeed was the case showing that even forecasts of near global scale temperatures can go wrong.

Mean Sea Level Pressure

As was stated above, MSLP is not directly affected by changes in radiative forcing following a volcanic eruption but may, due to dynamical effects, be indirectly influenced by changes in atmospheric temperature [*Robock and Mao*, 1992; *Graf et al.*, 1993; *Robock and Mao*, 1995]. Changes atmospheric flow patterns induced by changes in temperature (and revealing themselves in changes in MSLP) may further enhance or dampen the volcanic temperature signal. The ensemble-mean MSLP anomaly response in the northern hemisphere winters following El Chichón and Pinatubo is shown in fig. 7, together with the observed MSLP anomalies and the ensemble probabilities of lower than average MSLP. The patterns of MSLP are more complicated than the surface temperature patterns, reflecting the indirect nature of the forcing of the pattern.

There are, however, some features that are predicted by the model. Following El Chichón, the model predicts a positive NAO-like pattern of MSLP in the North Atlantic region with lower pressure in the polar-regions and higher pressure further south. This pattern is approximately what happened in reality and is, in part, responsible for the pattern of warming predicted by the model (fig. 4). However, the amplitude of the pattern is significantly larger in reality and results in a stronger observed winter warming than was predicted by the model. In the Pacific basin, the model predicts lower than average pressure in a pattern that is similar to the Pacific North American (PNA) pattern more generally associated with an El Niño event. This is indeed what happened in reality, although separating the component of the observed signal which is a result of El Niño from that resulting from El Chichón is difficult using the model experiments used here.

Despite the greater radiative forcing following Pinatubo, the MSLP response is paradoxically weaker than in the case of El Chichón. In reality, there was higher than average pressure over western Europe in the winter of 1991-2 which resulted in a north-south dipole in temperature anomalies (fig. 4). The model does predict some higher than average MSLP in the North Atlantic but the pattern is shifted too far to the west. Again the PNA pattern is evident in the observations (possibly associated with the weak El Niño event at this time), but was not predicted by the model in this case.

The general conclusion that may be drawn is that MSLP is less predictable than SAT following a volcanic eruption. This is not surprising as MSLP is not directly effected by the changing in radiative forcing that the aerosol cloud induces. The corollary is that many associated variables such as the position and strength of the storm track, may also be less predictable, although it is clearly a matter of future research to whether this really is the case.

Further inferences that may be drawn from these experiments

Before concluding it is possible to address some further questions about the response of the climate system following volcanic eruptions that have been raised.

Can volcanoes trigger El Niño events?

It has been suggested that large volcanic eruptions may trigger El Niño events in the tropical Pacific [*Hirono,*1988], although this possibility has been questioned by *Robock et al.* [1995], *Robock and Free* [1995] and *Self et al.* [1997]. The large 1982/83 El Niño followed the eruption of El Chichón, and there was a smaller El Niño event at the time of Pinatubo. As was pointed out by *Robock* [2000], El Niño events occur naturally every 3-7 years, so it is easily possible that the coincidence of the events with the volcanic eruptions is simply chance. Theories of El Niño suggest that there must be some “pre-conditioning” of the state of the tropical Pacific ocean prior to the onset of an El Niño, but that chance atmospheric fluctuations can then “tip the balance” and set the system going towards an El Niño. Hence while the suggestion may, at first sight, seem rather outlandish, there is a potential mechanism by which a volcanic eruption may result in a change in e.g. SSTs or tropical trade winds and an El Niño event that may not have occurred in the absence of the eruption, may result.

It is clear from the model experiments here that, for arbitrarily selected ocean initial conditions, there is no significant bias towards the occurrence of El Niños or La Niñas following the eruption of El Chichón and Pinatubo. HadCM3 has a relatively realistic ENSO cycle, and the model has been used in studies of ENSO response to global warming [*Collins,* 2000] and in ENSO predictability studies [*Collins et al.,* 2002]. Figure 8 shows NINO3 SST anomalies (a good indicator of El Niño) from the ensemble of simulations following the two volcanic eruptions. If the model simulated a bias in the ensemble mean towards warmer or cooler NINO3 anomalies following either eruption, then this would indicate a strong link between volcanoes and El Niño. The model does simulate El Niño and La Niña events following both eruptions, but there is approximately an equal number of each type. These simulations support the analysis of *Robock et al.*

[1995], *Robock and Free* [1995] and *Self et al.* [1997] that volcanoes do not, in general, trigger El Niño (or La Niña) events. However the question of whether an eruption may amplify or damp a warm or cold event when the ocean state is pre-conditioned to follow such a path is still open.

Can volcanoes halt global warming?

Because of their cooling effect on global temperatures, volcanic eruptions have the potential to temporarily halt the global warming signal coming (principally) from the continuing increase in greenhouse gases from anthropogenic sources. This may alleviate the effects of global warming and confuse the global political debate on the mitigation of and adaptation to climate change [*Hyde and Crowley,* 2000]. The relatively large number of ensemble members in the simulations of El Chichón and Pinatubo used in this study allows a more robust estimate of the global effects of the eruptions minimizing the noise of natural climate fluctuations. The ensemble mean globally averaged land and ocean temperature from the experiments is shown in fig. 9, together with the +/- 2 standard deviations from the 20 ensemble members highlighting the range of variability that would be found in the observations or in a single ensemble member. The observations (dotted line in fig. 9) lie within these bounds indicating that the model response to the eruptions and to the longer term anthropogenic forcing is realistic (see *Stott et al.* [2000]) for a more detailed validation of decadal trends). Hence it is possible to use the decadal mean cooling in the experiments (formed by averaging the detrended ensemble mean temperature response) in estimating the potential for volcanoes to temporarily halt global warming.

The model estimates the decadal global mean cooling attributable to El Chichón was 0.04°C and that attributable to Pinatubo was 0.12°C. The ratio of the former to the latter is 3, which scales remarkably well with relative amounts of stratospheric SO_2 being 20*Mt*/7*Mt. Stott and Kettleborough* [2002] estimate that the temperature rise in the decade 2020-30 due to anthropogenic warming alone to be 0.4 to 1.2°C in comparison to 1990-2000 levels. This is the 5-95% range arising from both from uncertainty in future levels of greenhouse gases and from uncertainty in the climate sensitivity and rate of heat uptake by the ocean in the model. Assuming the anthropogenic trend to be approximately linear in this period (a reasonanble assumption - see fig. 1 of *Stott and Kettleborough* [2002]) then the 5-95% range of global temperatures in the decade 2005-15 will be 0.2 to 0.6°C. Taking the lower of these ranges it would take a volcanic eruption with approximately twice the global cooling signal of Pinatubo to mask the anthropogenic signal in the decade 2005-15. Taking a more realistic value for the projected anthropogenic trend (e.g. 0.4°C) it would take something like a x4 Pinatubo to mask the trend. *Hyde and Crowley,* [2000] calculate (from ice core records) that the probability of such an eruption is less than a few percent. These order of magnitude calculations suggest that it is highly unlikely that a volcanic eruption could completely mask the anthropogenic signal in the coming decade. However, nature never ceases to amaze us and only time will tell.

How robust is winter warming?

The mechanism for volcanic winter warming phenomena was first elucidated by *Robock and Mao* [1992] and is discussed extensively by *Robock* [2000]. Following an eruption the tropical stratosphere warms and this increases the pole to equator temperature gradient at upper levels. The dynamical balance of the atmosphere is such that this increased gradient leads to an increase in the upper level zonal jet speed (via thermal wind balance). The effects of this acceleration of the polar jet are felt at the surface where warmer maritime air is advected over the cold continental regions. Various refinements to this explanation involve the excitation of atmospheric modes of variability such as the NAO, which is related to the jet speed in the North Atlantic region, and feedbacks involving the propagation of atmospheric waves. There is also historical observational evidence [*Groisman,* 1992] that warmer winters generally follow volcanic eruptions.

As was the case with ENSO, modes of variability such as the NAO exhibit year-to-year variations independent of volcanic eruptions and the occurrence of high NAO (and stronger jet stream) years following El Chichón and Pinatubo might easily be due to chance climate fluctuations. Figure 9 shows the observed and simulated NAO behaviour for the two winters following both eruptions. In the first winter, the model simulates a bias towards a high NAO with the bias being stronger in the case of El Chichón. In the second winter following the eruptions the model mean NAO is close to climatology indicating no impact of the volcanic forcing on the NAO. In all cases the observed NAO was higher than average, but well within the range of variability suggested by climatology. The key point here is that the displacement of the mean of the NAO distribution following the eruptions is not particularly large, so that while the winter warming mechanism clearly operates in the model, the magnitude of the response would not be enough to issue an unequivocal forecast of higher NAO values and warmer winters following an eruption. The apparent agreement with the sign (but not the magnitude) of NAO response in the modeling studies of El Chichón and Pinatubo (e.g. *Kirchner et al.* [1999]) may be fortuitous. In these experiments 4 out of 20 ensemble members have a negative NAO projection following El Chichón and 9 out of 20 following Pinatubo. Of course the model may be unduly insensitive to the forcing, but this is a matter for further research.

Discussion

Large explosive volcanic eruptions may have a devastating impact on the local population and natural environment. However, for eruptions that inject a large amount of SO_2 into the stratosphere, the global climate impacts paradoxically allow the potential for climate forecasts which may be of benefit to society. In this paper, the potential for such forecasts has been quantified by examining hindcasts of climate following the eruptions of El Chichón (1982) and Pinatubo (1991).

Because climate forecast are inherently probabilistic, climate predictability only arises when a phenomena can significantly modify the probability density function (PDF) of some climate variable. Eruptions of the size of El Chichón and Pinatubo can significantly shift the PDFs of climate variables such as surface air temperature and mean sea level pressure, and the shifts are more robust for large continental scale seasonal averages. Care should however be taken in utilizing such climate forecasts as the volcanic signal can easily be contaminated or even completely obscured by the “noise” of natural climate fluctuations which occur regardless of the eruption.

It is clear however, that even for the simple verification presented here, there is some utility in making a forecast following the next big eruption. Also, the skill scores used in this study are rather crude and there is a danger that they may mask some aspect of the hindcasts that, in fact, has very high skill e.g. the prediction of extreme low temperatures. Forecast verification should always be a user driven exercise as users are often interested in different climate variables, different seasons and may also be accepting of different levels of accuracy. Only the end-user of the forecasts can really judge how useful a forecast was or might be in the future.

It is also worth putting the prediction of the climatic impacts of a volcanic eruption in the context of other climate forecasting efforts. As was stated in the introduction, the main predictable climate phenomena is the El Niño Southern Oscillation (ENSO), which has near global impact but the ENSO signal only affect regions such as Europe only weakly or during large ENSO events [*Mathieu et al.,* 2002]. Two key advantages of volcanic forecasts in comparison with ENSO forecasts are that volcanic forecasts may be of use in geographical regions remote from ENSO influence, and that ENSO is only predictable (on average) for a few seasons into the future [*Collins et al.,* 2002] whereas the volcanic dust cloud may persist for many years providing useful predictability. In addition, forecasts of other climate phenomena such as the North Atlantic Oscillation (NAO) are in their infancy and may, perhaps, never even be realized [*Collins,* 2002]. Volcanoes may yet prove to be a useful addition to the armory of the seasonal climate forecaster.

What is clear is that there should be continued effort in observing, modeling and understanding the climate impacts of volcanic eruptions. In addition, it may perhaps be wise for forecasting centers to develop the capacity to operationally forecast the impact of the next big eruption. This should include developing the ability to adequately simulate stratospheric dynamics and to transport sulphate aerosol from the source region. Because of the potential contamination of the volcanic signal by natural climate fluctuations, it is also be important to start forecasts from initial conditions appropriate to the current observed state of the climate system (principally the ocean).

Acknowledgements

Many thanks go to the organizers of the Chapman Conference on Volcanoes and the Earths Atmosphere who provided travel support for the author to attend the meeting. The author has benefited greatly from conversations with Ellie Highwood, Gareth Jones and Peter Stott who also provided the experimental details for the model integrations. This work was supported by the COAPEC programme of the UK Natural Environment Research Council.

References

Andrononva, N. G., E. V. Rozanov, F. Yang, M. E. Schlesinger and G. L. Stenchikov, Radiative forcing by volcanic aerosols from 1850 to 1994. *J. Geophys. Res., 104,* 16,807-16,826, 1999.

Basnett, T. and D. E. Parker, Development of the global mean sea level pressure data set, *Hadley Centre Technical Note, 79,* p61, 1997.

Bluth, G. J. S., S. D. Doiron, S. C. Schnetzer, A. J. Kruger and L. S. Walter, Global tracking of the SO_2 clouds from the June 1991 Mount Pinatubo eruptions, *Geophys. Res. Lett., 19,* 151-154, 1992.

Collins, M., Understanding Uncertainties in the response of ENSO to Greenhouse Warming, *Geophys. Res. Letts., 27,* 3509-3513, 2000.

Collins, M., D. Frame, B. Sinha, and C. Wilson, C., How far ahead could we predict El Niño? *Geophys. Res. Letts., 29,* 10.1029/2001GL013919, 2002.

Collins, M. and M. R. Allen, On assessing the relative roles of initial and boundary conditions in interannual to decadal climate predictability *J. Climate,* in press, 2002.

Collins, M., S. F. B. Tett, and C. Cooper, The internal climate variability of HadCM3, a version of the Hadley Centre coupled model without flux adjustments. *Clim. Dyn., 17,* 61-81, 2001.

Gordon, C., C. Cooper, C. A. Senior, H. Banks, J. M. Gregory, T. C. Johns, J. F. B. Mitchell, and R. A. Wood, The simulation of SST, sea ice extents and ocean heat transport in a version of the Hadley Centre coupled model without flux adjustments. *Clim. Dyn., 16,* 147-168, 2000.

Graf, H.-F., I. Kirchner, A. Robock, and I. Schult, Pinatubo eruption winter climate effects: Model versus observations, *Clim. Dyn., 9,* 83-91, 1993.

Groisman, P. Y., Possible regional climate consequences of the Pinatubo eruption: An empirical approach, *Geophys. Res. Lett., 19,* 1603-1606, 1992.

Hirono, M., On the trigger of El Niño-Southern Oscillation by the forcing of early El Chichón volcanic aerosols, *J. Geophys. Res., 93,* 5364-5384, 1988.

Houghton, J. T., Y. Ding, D. J. Griggs, M. Noguer, P. J. van der Linden, X. Dai, K. Maskell, and C. A. Johnson (Eds.), *Climate Change 2001: The Scientific Basis. Contribution of Working Group I to the Third Assessment Report of the Intergovernmental Panel on Climate Change,* Cambridge University Press, 2001.

Hurrell, J. W., Decadal trends in the North Atlantic Oscillation: Regional temperatures and precipitation, *Science, 268,* 676-679, 1997.

Jones, P. D., Hemispheric surface air temperature variations: A reanalysis and update to 1993, *J. Clim., 7,* 1794-1802, 1994.

Kirchner, I., G. L. Stenchikov, H.-F. Graf, A. Robock, and J. C. Antuna, Climate model simulations of winter warming and summer cooling following the 1991 Mount Pinatubo volcanic eruption, *J. Geophys. Res., 104,* 19,039-19,055, 1999.

Lorenz, E. N., The physical basis of climate and climate modeling, in *Climate Predictability, GARP Publication Series,* 132-136, 1975.

Lorenz, E. N., Atmospheric predictability experiments with a large numerical model, *Tellus, 34,* 505-513, 1982.

Mao, J. and A. Robock, Surface air temperature simulations by AMIP general circulation models: Volcanic and ENSO signals and systematic errors. *J. Clim., 11,* 1538-1552, 1998.

Mathieu, P-P., R. T. Sutton, B. Dong, and M. Collins, M., Predictability of winter climate over the North Atlantic European region during ENSO events. *In preparation.*

Robock, A. and M. P. Free, Ice cores as an index of global volcanism from 1850 to the present, *J. Geophys. Res., 100,* 11,549-11,567, 1995.

Robock, A. and Y. Liu, The volcanic signal in the Goddard Institute for Space Studies three-dimensional model simulations, *J. Clim., 7,* 44-55, 1994.

Robock, A. and J. Mao, Winter warming from large volcanic eruptions, *Geophys. Res. Lett., 19,* 2405-2408, 1992.

Robock, A. and J. Mao, The volcanic signal in surface temperature observations, *J. Clim., 8,* 1086-1103, 1995.

Robock, A. and M. Matson, Circumglobal transport of the El Chichón volcanic dust cloud, *Science, 221,* 195-197, 1983.

Robock, A., K. E. Taylor, G. L. Stenchikov, and Y. Liu, GCM evaluation of a mechanism for El Niño triggering by the El Chichón ash cloud, *Geophys. Res. Lett., 22,* 2369-2372, 1995.

Robock, A., Volcanic Eruption and Climate, *Rev. in Geophys., 38,* 191-219.

Robock, A., Stratospheric Forcing Needed for Dynamical Seasonal Prediction, *Bull. Amer. Met. Soc., 82,* 2189-2191, 2001.

Sato, M., J. E. Hansen, M. P. McCormick, and J. B. Pollack, Stratospheric aerosol optical depths, 1850-1990, *J. Geophys. Res., 98,* 22,987-22,994, 1993.

Self, S., M. R. Rampino, J. Zhao, and M. G. Katz, Volcanic aerosol perturbations and strond El Niño events: No general correlation, *Geophys. Res. Lett., 24,* 1247-1250, 1997.

Stott, P. A., S. F. B. Tett, G. S. Jones, M. R. Allen, J. F. B. Mitchell and G. J. Jenkins, External control of 20th century temperature by natural and anthropogenic factors, *Science, 290,* 2133-2137, 2000.

Stott, P. A. and J. A. Kettleborough, Origins and estimates of uncertainty in predictions of twenty-first century temperature rise, *Nature, 416,* 723-726, 2002.

Stenchikov, G. L., I. Kirchner, A. Robock, H.-F. Graf, J. C. Antuna, R. G. Grainger, A. Lambert and L. Thomason, Radiative forcing from the 1991 Mount Pinatubo volcanic eruption. *J. Geophys. Res., 103,* 13,837-13,857, 1998.

Stowe, L. L., R. M. Carey, and P. P. Pellegrino, Monitoring the Mount Pinatubo aerosol layer with NOAA 11 AVHRR data, *Geophys. Res. Lett., 19,* 159-162, 1992.

Strong, A. E., Monitoring El Chichón aerosol distribution using NOAA-7 satellite AVHRR sea surface temperature observations, *Geofis. Int., 23,* 129-141, 1984.

Tables

Year	Season	Skill of predictions of > average SAT	Skill of predictions of < average SAT	Skill of prediction of sign of SAT anomalies
1982	SON	20% (24%-38%)	67% (73%-85%)	44% (46%-66%)
1982-3	DJF	49% (43%-65%)	62% (49%-68%)	53% (46%-66%)
1983	MAM	39% (29%-48%)	66% (52%-77%)	50% (42%-59%)
1983	JJA	19% (20%-35%)	73% (75%-88%)	44% (46%-68%)
1983	SON	16% (16%-34%)	62% (67%-81%)	32% (37%-63%)
1983-4	DJF	42% (31%-56%)	63% (50%-73%)	52% (41%-64%)
1984	MAM	33% (32%-50%)	53% (54%-73%)	44% (45%-61%)
1984	JJA	24% (30%-41%)	58% (62%-77%)	42% (47%-60%)
1984	SON	41% (46%-60%)	52% (49%-70%)	48% (41%-61%)
1984-5	DJF	52% (63%-75%)	22% (27%-41%)	34% (42%-59%)

Table 1: Simple verification scores for the hindcasts of seasonally averaged surface air temperature following the eruption of El Chichón. Columns 1 and 2 indicate the year and season of the verification. Column 3 is the percentage of 5ºx5º grid boxes in which the temperature was greater than average and the model predicted that this would be the case. Column 4 is the percentage of 5ºx5º grid boxes in which the temperature was less than average and the model predicted that this would be the case. Column 5 is the combined skill score for anomalies of both sign i.e. the percentage of grid boxes in which the correct sign of temperature anomaly was predicted. Figures in brackets show the range of "perfect model" skill scores obtained by substituting each member of the ensemble as the truth and indicates how random variations in climate can affect the forecast verification. An entirely random forecast would have an average skill of 50% in columns 3-5.

Year	Season	Skill of predictions of > average SAT	Skill of predictions of < average SAT	Skill of prediction of sign of SAT anomalies
1991	SON	49% (38%-68%)	60% (50%-70%)	55% (43%-67%)
1991-2	DJF	35% (25%-53%)	65% (59%-80%)	48% (45%-67%)
1992	MAM	13% (15%-35%)	66% (74%-84%)	41% (45%-66%)
1992	JJA	9% (10%-20%)	86% (87%-96%)	62% (56%-76%)
1992	SON	14% (15%-28%)	77% (79%-88%)	64% (48%-68%)
1992-3	DJF	22% (26%-48%)	55% (62%-82%)	38% (47%-65%)
1993	MAM	19% (21%-33%)	69% (72%-81%)	45% (43%-64%)
1993	JJA	15% (22%-38%)	64% (71%-80%)	41% (46%-67%)
1993	SON	25% (29%-54%)	58% (58%-77%)	47% (46%-67%)
1993-4	DJF	45% (44%-65%)	46% (42%-65%)	46% (43%-59%)

Table 2: As in table 1 but for the Pinatubo eruption.

Year	Season	Skill of prediction of sign of SAT anomalies	Year	Season	Skill of prediction of sign of SAT anomalies
1982	SON	43% (34%-81%)	1991	SON	65% (43%-75%)
1982-3	DJF	58% (41%-74%)	1991-2	DJF	34% (32%-83%)
1983	MAM	60% (41%-70%)	1992	MAM	42% (35%-83%)

1983	JJA	45% (45%-77%)	1992	JJA	82% (55%-97%)
1983	SON	28% (38%-70%)	1992	SON	78% (44%-89%)
1983-4	DJF	69% (40%-68%)	1992-3	DJF	27% (39%-75%)
1984	MAM	55% (42%-72%)	1993	MAM	50% (33%-83%)
1984	JJA	45% (39%-77%)	1993	JJA	55% (40%-83%)
1984	SON	55% (24%-70%)	1993	SON	52% (37%-69%)
1984-5	DJF	18% (27%-72%)	1993-4	DJF	64% (32%-73%)

Table 3: Verification skill scores for the predicted sign of temperature anomalies in overlapping regions of size 25ºx25º longitude-latitude (as in tables 1-2), i.e. the percentage of 25ºx25º regions in which the sign of the observed temperature was correctly predicted by the model. The figures in brackets show the range of scores obtained by substituting each ensemble member for the observations.

Figures

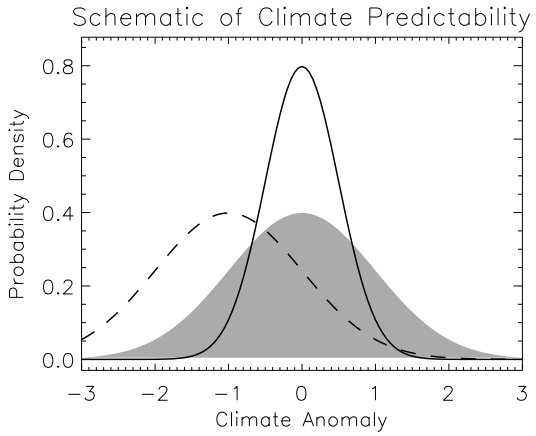

Figure 1: Schematic diagram highlighting how climate predictability may arise. The grey shading represents the climatological probability density function (PDF) of e.g. winter mean temperature anomalies over a region such as Western Europe. It is not possible to predict the precise value of winter mean temperature – there is always a large random component and all climate forecasts are probabilistic in nature. The potential for prediction comes when there is some significant perturbation to the climatological PDF. If the future PDF is narrower than the climatological PDF (solid line) then there is an increase in the probability of normal conditions and a decrease in the probability of extreme warm or cold temperatures. This will occur if the spread on initially near-by trajectories is smaller than the mean climatological distance between different states. If the future PDF is displaced with respect to the normal conditions, this introduces a bias and, in the example shown (dashed line), results in an increase in the probability of colder than average temperatures and a decrease in the probability of warmer than average temperatures. This may happen following a volcanic eruption.

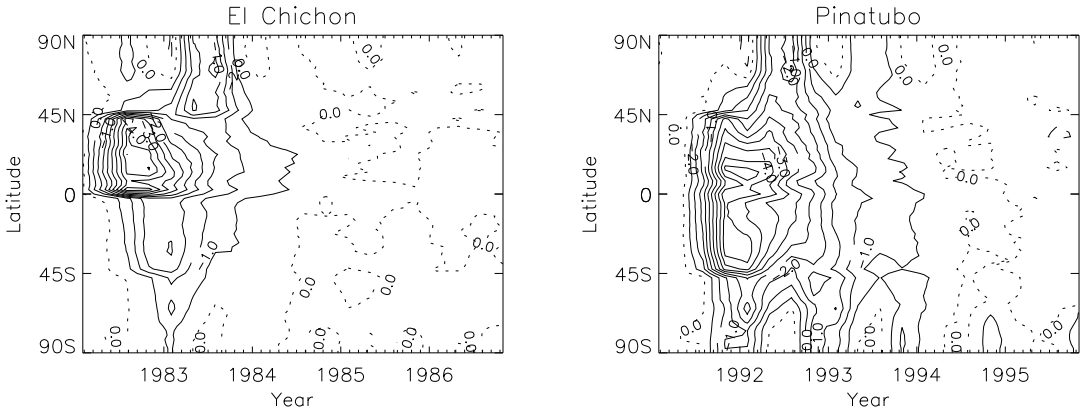

Figure 2: The latitude-time distribution (averaged over longitude) of the net tropopause radiative forcing resulting from the introduction of stratospheric aerosol into the HadCM3 coupled atmosphere-ocean model following the eruption of El Chichón (left panel) and Pinatubo (right panel). Aerosol optical depths are taken from an updated version of *Sato et al.* [1993] and are introduced uniformly in longitude in four latitude bands each with a width of 45° latitude. The contour interval is 0.5 Wm^2 and negative contours (indicating a cooling influence) are drawn as solid lines and the zero contour is drawn as the dotted line.

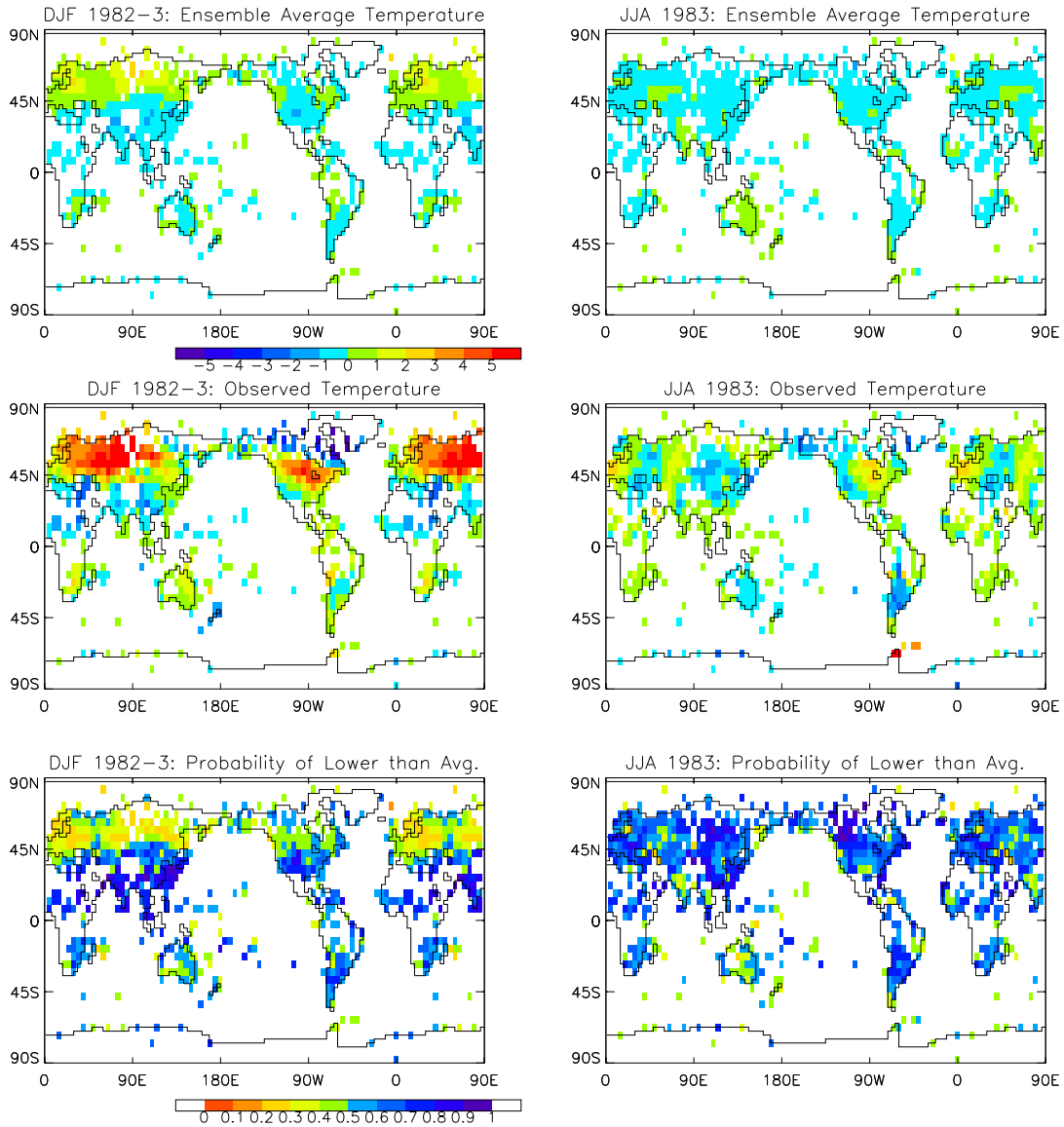

Figure 3: The modeled and observed seasonally averaged land surface air temperature in the winter (December to February – DJF) and summer (June-August – JJA) following the eruption of El Chichón. The upper panels show the mean of 20 simulations of the eruption made using version three of the Hadley Centre coupled atmosphere-ocean model. Model temperatures are interpolated onto the same grid as the Jones et al. observations (middle panels) and regions in which there are no observations are also blanked in the model. The lower panels show the probability of cooler than average temperatures computed from the 20 ensemble members.

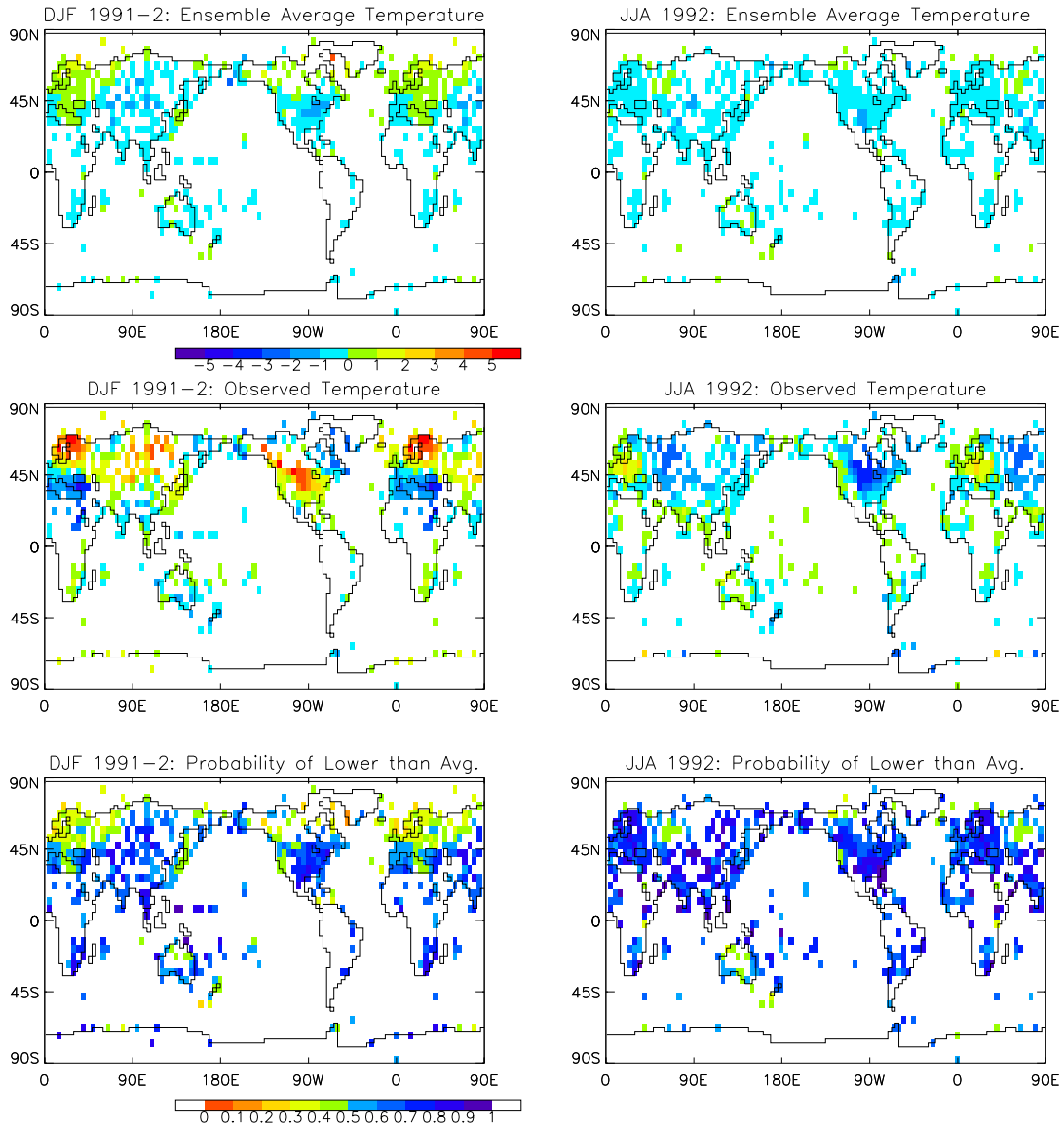

Figure 4: As in fig. 3 but for the eruption of Pinatubo.

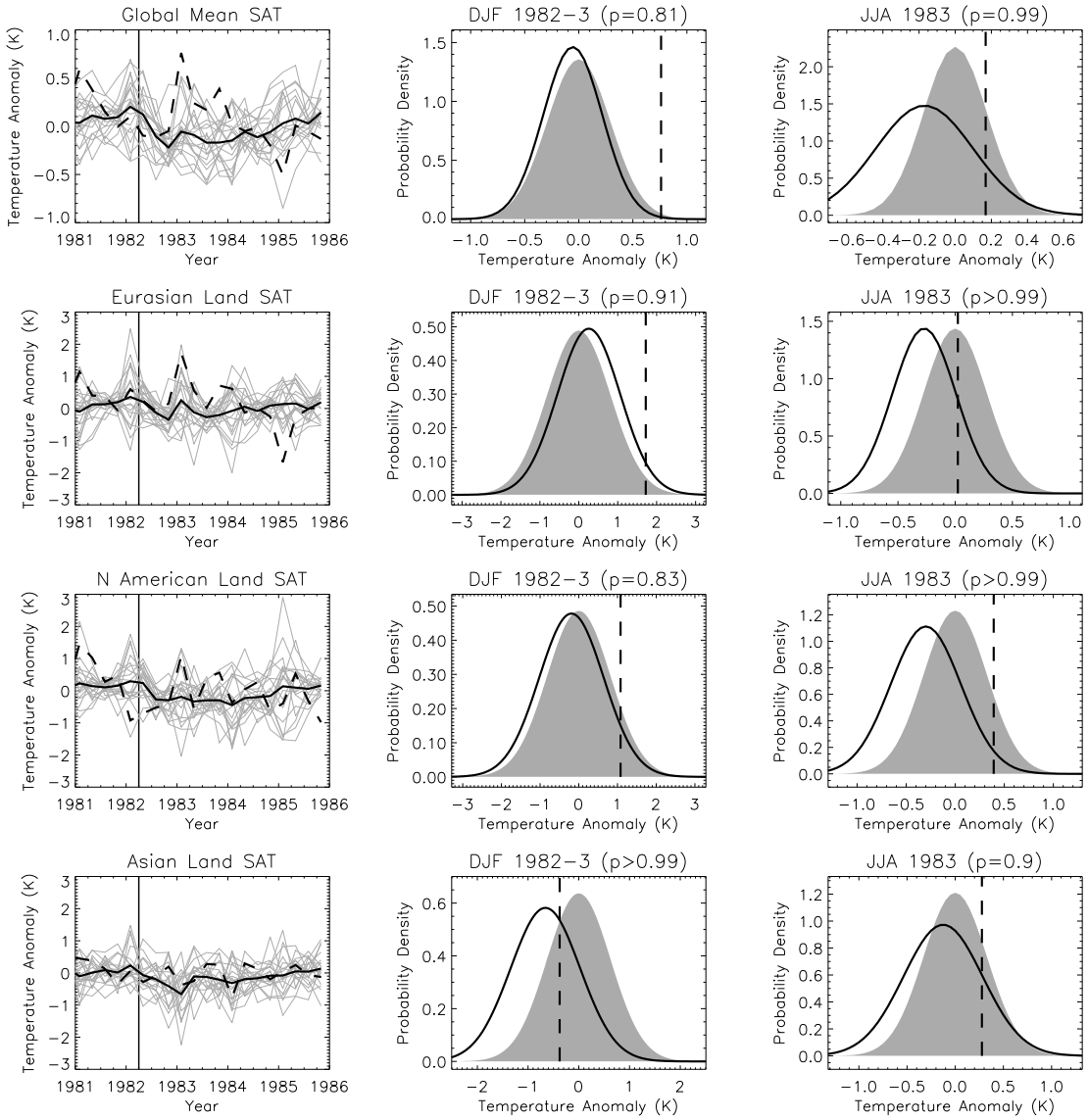

Figure 5: Time series and probability density functions (PDFs) of large-scale averages of modeled and observed seasonal temperature anomalies following the eruption of El Chichón. The left panels show time series of modeled temperatures from each ensemble member (grey lines), the mean of all the ensemble members (thick black line) and the observations (thick dashed line). The vertical black line indicates the time of the eruption. Anomalies are computed with respect to a climatology averaged over the five years prior to the year of the eruption. The middle panels show the PDF of the model winter (DJF) climatology (grey shading) computed using 2000 years of control simulation with fixed greenhouse gases and aerosols. The thick black line shows the "forecast PDF" i.e. the PDF computed from the ensemble of 20 simulations of El Chichón and would be the type of PDF that would be used to make a forecast in an operational system. The vertical dashed line shows the value of the observed anomaly for winter 1982-3. The figure in brackets in the plot title of the form 'p=' is the t-test probability of the mean of the forecast PDF being statistically different from the mean of the climatological PDF. The right panels show the same for summer (JJA) temperature anomalies. Four large-scale averages are shown; global mean land (upper row), Eurasian land (0E-180E, 30N-80N) – second panel), North Americal land (160W-50W, 20N-70N – third panel) and Asian land (60E-120E, 10N-40N – final panel).

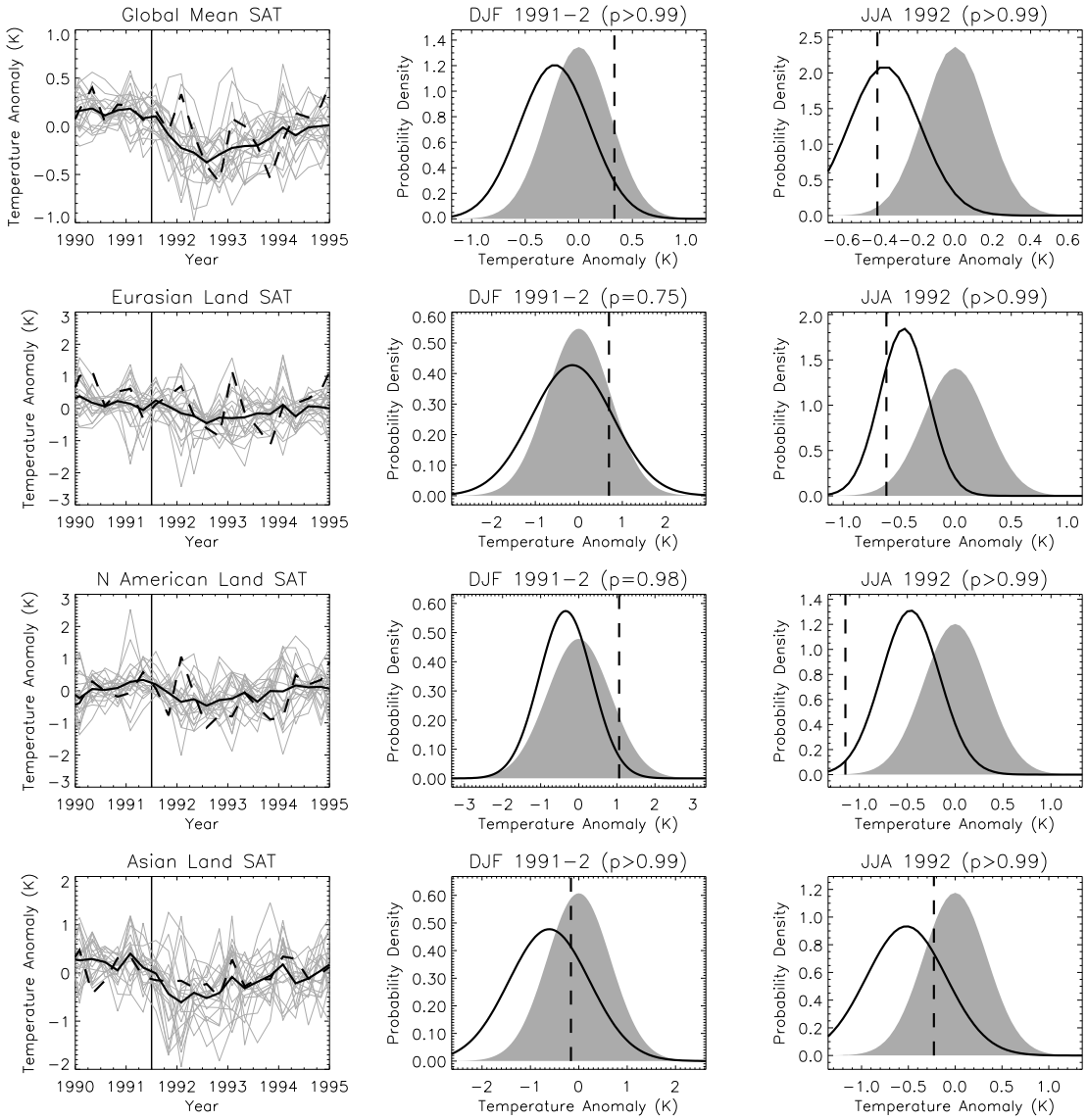

Figure 6: As in figure 5 but for large scale averages of temperature anomalies following Pinatubo.

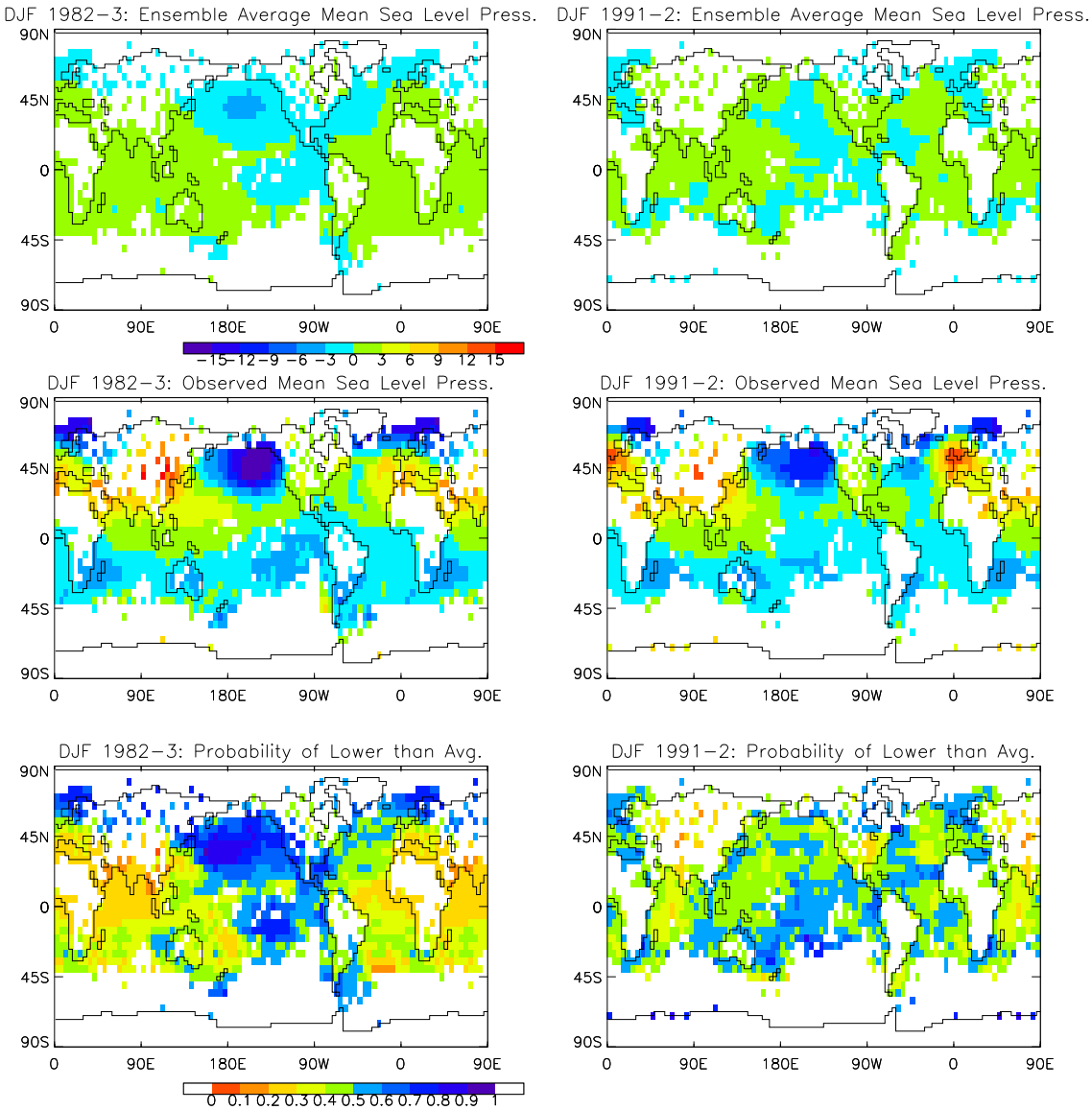

Figure 7: The simulated and observed Mean Sea Level Pressure (MSLP) anomalies in the winter seasons following El Chichón and Pinatubo. The convention is the same as that in figs. 3-4.

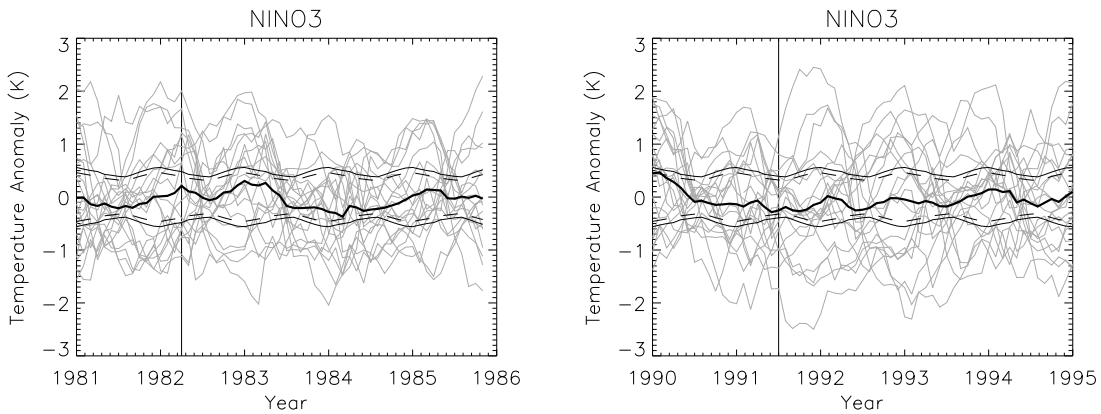

Figure 8: Simulated NINO3 anomalies (sea surface temperature anomalies averaged in the region 150W-90W, 5S-5N) following the eruption of El Chichón (left panel) and Pinatubo (right panel). NINO3 is a good indicator of El Niño and La Niña events. Individual ensemble members are shown in grey and the ensemble mean is shown in black. The thin black dashed and solid lines show the

95% and 99% probability limits for the ensemble mean. The model used in this study shows no strong bias towards the occurrence of either El Niño or La Niña events following a volcanic eruption.

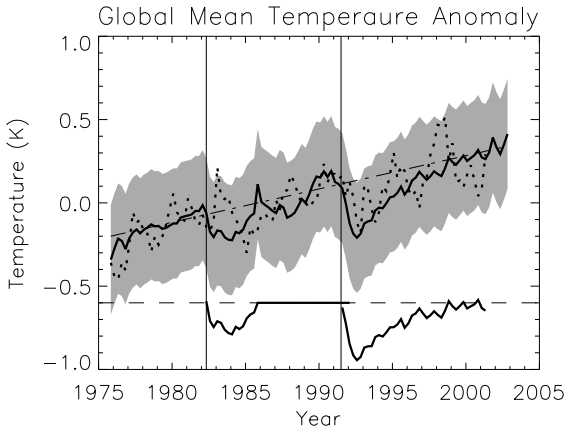

Fig 9: Global mean surface temperatures (land and ocean) from the ensemble mean of the model simulations (solid line) and the observations (dotted line). The shading shows the +/- 2 standard deviations of global mean temperature computed from the 20 ensemble members and highlight the range of possible “noise” in the observations or in a single ensemble member. The dashed line shows the linear trend from the anthropogenic forcing included in the simulations. The lower curves show the decadal volcanic signal with the trend removed (and offset by 0.6°C) to show the possible impact of volcanic eruptions on global temperatures. The simple analysis presented in the text suggests that it is highly unlikely that a volcanic eruption would mask the anthropogenic signal in the next decade.

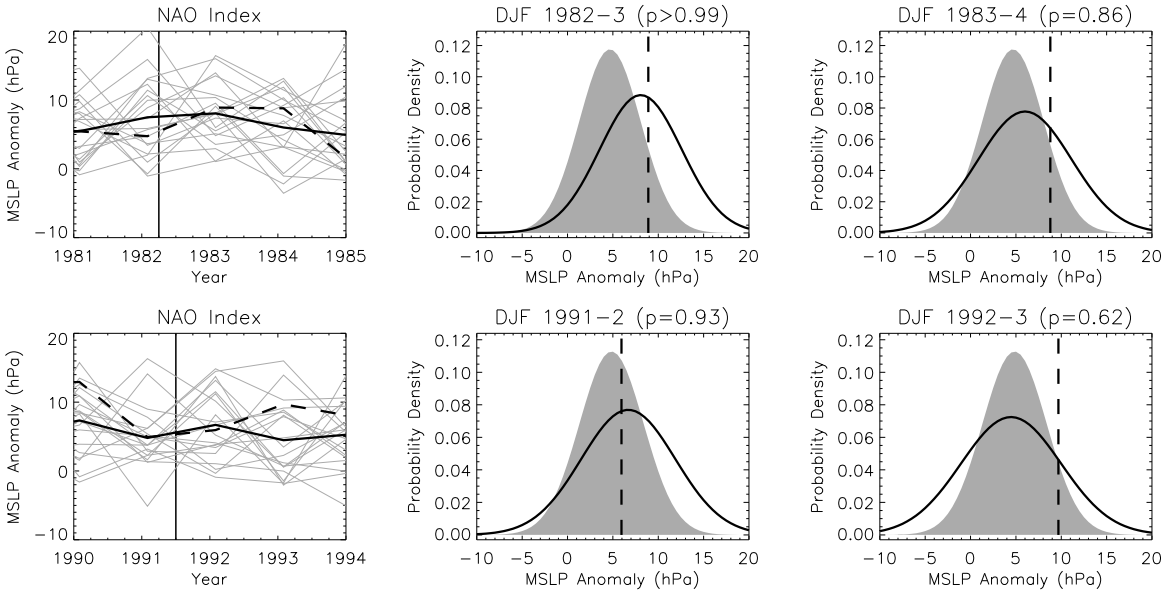

Fig 10: Time series and PDFs (similar to those in figs 5-6) of the North Atlantic Oscillation index following El Chichón and Pinatubo. The index is defined as the winter mean pressure averaged in the region 90°W-60°E, 20°N-55°N minus the pressure averaged in the region 90°W-60°E, 55°N-90°N This is different from the normal definition of the index [*Hurrel*, 1997] and allows a direct comparison of the magnitude of the pressure gradient (and hence the wind speed) between the model and the observations. It also reduces errors associated with station-based indices that may arise from systematic errors in the model NAO pattern. The left panel shows the ensemble mean (black line), the ensemble members (grey lines) and the observed (dashed line) NAO index. The

middle and right panels show the climatological PDF (grey shading), the enseble PDF (black line) and observed value of the NAO (dashed line).